Performance of Air Foam Flooding under Low Frequency Vibration

Pu Chunsheng[1,2], Zheng Liming*[1], Liu Jing[1], and Xu Jiaxiang[1]

[1] School of Petroleum Engineering, China University of Petroleum (Eastern China), Qingdao, China
[2] State Key Laboratory of Heavy Oil, Qingdao, China

ABSTRACT

Foam injection is widely applied in amounts of fields to drilling, production, and formation protection. Sometimes, the application result is disappointing, which is caused by the failure of bubble generation in foam flooding. Therefore, it is necessary to seek ways for improving the performance of foam injection. An increased disturbance to the stratum, like the vibration caused by a seismic oil recovery technique, would be helpful. In the current work, the seepage of air foam in porous media under low frequency (LF) vibration is analyzed with experiments and an investigation of bubble creation/destruction rate change is carried out using mathematical modeling. The resistance factor of foam flooding under indoor vibration increases by 1.5 times and the valid time is obviously extended compared with when no vibration is used. The optimal vibrating acceleration and frequency of 0.7 m/s^2 and the natural frequency of the cores-nearby of 18 Hz are achieved in the indoor experiments. Under vibration, the bubble generation rate increases, while bubble break rate by internal expansion or by gas diffusion and transfer decreases. An interesting phenomenon is also observed, which might develop a power level formula between the initially defined dimensionless MRF (maximum foam flooding resistance factor) and dimensionless DMRF (duration of maximum foam flooding resistance factor). The power product and sum of the power exponents of the above formula both equal approximately to 1. With the assistance of LF vibration, the increase of security, adaptability, and efficiency in foam injection may improve the reservoir recovery and extend its application.

Keywords: Air Foam Flooding, Low Frequency Vibration, Resistance Factor, Foam Stabilization, Low Permeable Reservoir

INTRODUCTION

Air foam flooding [1-2] and low frequency vibration oil extraction technology [3-5] (also known as the artificial seismic oil recovery technology) are widely applied to low permeability reservoirs. For their wide adaptability and better performance in dead oil displacement inside the fine pores or throats, the development efficiency could be improved. The gas source in air foam flooding is free and convenient to be obtained. The low frequency (LF) vibration is of a large action radius due to its weak attenuation when transmitting in porous media, and more wells could share the running cost. The low cost of air foam flooding and LF vibration oil extraction technology is attractive for application in oilfield.

However, low efficiency and disappointing economy effect were sometimes caused by the failure of bubble generation in foam flooding, which had caused a block in pilot tests. Furthermore, the safety concerns might be a key factor, even though foam injection had been widely applied and is relatively inexpensive. It is necessary to improve the performance of foam injection. Therefore, an increased disturbance to the stratum, like the vibration caused by LF vibration oil extraction technology, would be helpful to increase the bubble generation.

LF vibration oil extraction technology improves oil recovery through the following mechanisms [6-8]: (a) the absolute permeability is increased, for the capillary forces inside matrix and the particle blocking inner pore throats are reduced; (b) the seepage rate is improved, with the decrease in the viscosity of crude oil, the increase in hydrophilicity on rock surface, and the additional driving force added by vibrating; (c) the residual oil saturation is reduced and oil recovery is enhanced due to the increase in the detachment of crude oil in die pores and around the rock surface.

Air foam flooding mechanisms for enhancing oil recovery mainly include the following [9-11]: (a) the sweep efficiency is expanded, for the high permeable layers or seepage channels are plugged to achieve oil displacement in low permeability layers or bypassed throats; (b) the water-oil mobility ratio is increased on account of the higher foam viscosity; (c) the reservoir energy is increased and a driving force in the upper layer is generated, with the injection of gas; (d) the additional effect of chemical flooding is achieved, with the main components of foam system being surfactants as well.

Researches on foam under vibration were conducted mainly on static foam performance without porous media and wave propagation in foam systems [12-15], indicating an improvement in foam behavior with the impact of the wave.

The static foam performance includes foaming volume, the half-time of deposition, interfacial tension, compressibility, strain rate, etc. Wave propagation in foam systems includes flooding model, wave velocity, energy absorption, etc. However, there was less consideration in the real porous flow of foam with three phase coexistence. Therefore, what and how the foam performance change under low frequency vibration are investigated in wave loading experiments. Moreover, the variation in bubble creation/ destruction rate is analyzed in terms of the foam flooding model and elastic wave theory.

MATERIALS AND METHODS

Apparatus and Materials

As Figure 1 shows, the experiment apparatus is conducted on the horizontal vibration table (Figure 2) designed by the Physical & Eco-Chemical Technology and Engineering Center (PECTEC) of China University of Petroleum. The unconsolidated sand pack (25 cm length) is fixed on the horizontal vibration table with the foam liquid and gas injected into the inlet. A hand pump and a backpressure valve are used to establish the backpressure. The electronic balance, 2PB00C-type constant flux pump, gas flow meter, intermediate container, and electronic pressure gauge (0.001 MPa) are also used in the foam flooding.

The materials include distilled water, sodium chloride, calcium chloride, magnesium chloride, kerosene, AES (fatty alcohol-polyoxyethylene ether sodium sulfate), and hydrolyzed polyacrylamide (molecular weight of 10 million). The simulated formation water used in this study is $CaCl_2$ type and with a salinity of 40000 mg/L, according to the formation water of certain oil-field in Ordos basin. The sand is quartz sand with a uniform size, 80-mesh, and good abrasion. After filling and compaction in the unconsolidated sand pack, the sand is low permeable for about 30×10^{-3} μm^2.
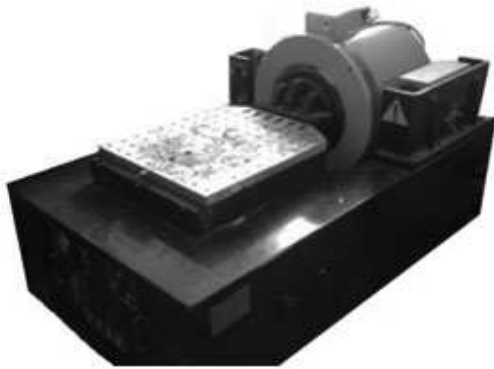
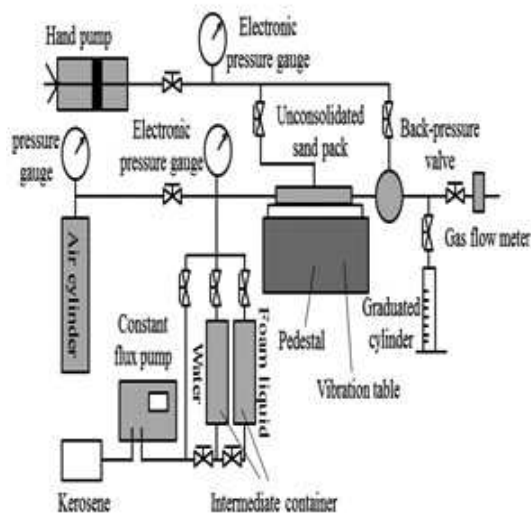**Figure 1: Indoor experimental device for low frequency vibration**

Figure 2: A schematic of the experimental workflow and apparatus

Experiment Procedure

Foam liquid, with an agent concentration of 0.5%, and air are injected into the unconsolidated sand pack repeatedly for three times. The total amount of foam liquid is 0.15 pore volume (PV) and gas-liquid volume ratio under the entrance pressure is 3:1. The back pressure is 1.0 MPa. Once the foam liquid is injected, the vibration table begins to work with a sinusoidal motion in the horizontal direction. The flowing fluid is along the same direction with generated propagating wave.

The pressure drop of water drive before or after air foam injection, expressed as P_1 and P_2 respectively, are measured successively at 30 °C

and the same flow rate. The resistance factor K, defined as the ratio of pressure drops above ($K = P_2 / P_1$), is an important indicator to evaluate foam mobility in porous media [16-17]. Through the analysis of K versus time under different vibrating parameters, the performance change in the water plugging of air foam is revealed.

The evaluation of dynamic foam performance under vibration includes the influence of vibrating time, vibrating frequency, and acceleration. To explore the influence of vibrating time on the resistance factors of air foam flooding, vibrating time is changed for 1, 2, and 3 hrs. During the process containing foam injection and water displacement afterwards, vibration continues until the set time. The vibrating frequency and acceleration are kept 18 Hz and 0.4 m/s^2 respectively. Resembling the above, four samples were prepared with a vibrating frequency of 5, 10, 18, and 25 Hz to explore the influence of vibrating frequency, while the vibrating time and acceleration were kept 1 hr and 0.4 m/s^2 respectively. The influence of vibrating acceleration on foam flooding was conducted by setting the vibrating acceleration to 0.2, 0.4, 0.7, and 1.0 m/s^2, while the vibrating time and frequency were kept constant at 1 hr and 18 Hz respectively. In contrast, a sand sample was also foam flooded without vibration.

RESULTS AND DISCUSSION

Vibrating Time

Variation tendencies of resistance factor at different vibrating times are similar as shown in Figure 3. It is characterized by three stages, namely a sharply increasing stage, a stable stage, and a slowly decreasing stage. The first stage lasts for about 30-100 minutes before the resistance factor increases to a maximum value; the second stage remains for about 80-150 minutes in our experiments and then the resistance factor decreases gradually.
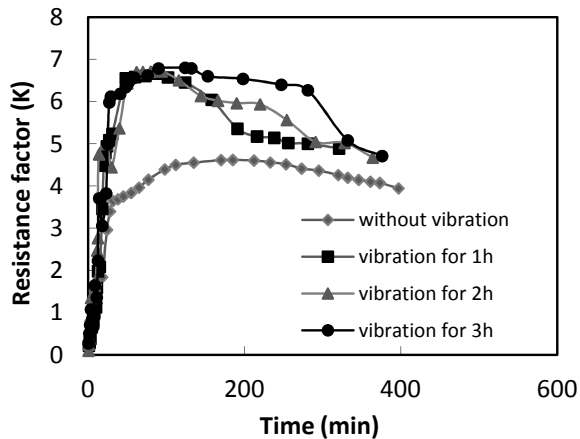
Figure 3: Influence of vibration time on resistance factor

At different vibrating times, the maximum resistance factor (MRF) is found approximately the same, which indicates that MRF and instant foaming speed are scarcely affected by the change of the whole vibrating time. However, the durations of maximum resistance factor (DMRF) in three experiments are different. Because the resistance factor is always changing over time and the maximum is an isolated point, DMRF is defined as the period in which resistance factor value is not less than a certain percentage of the MRF. The percentage chosen herein is 85%, because the value in the range of most samples is close to the MRF. The analysis of DMRF versus vibrating time is shown in Figure 4.
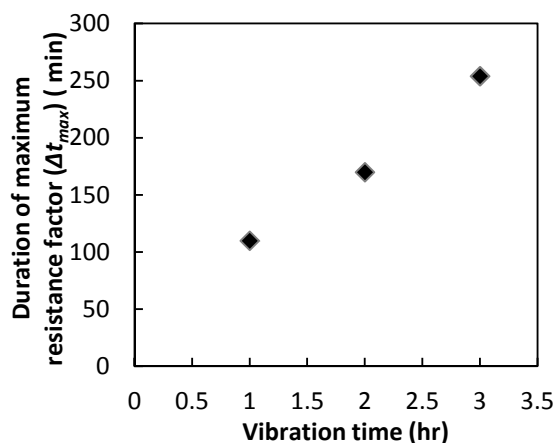

Figure 4: Duration of maximum resistance factor versus vibration time

The DMRF becomes larger as the vibrating time

is prolonged and the data in Figure 4 is linearly fitted by Equation 1:

$$\Delta t_{max} = 72 t_v + 34 \tag{1}$$

where, Δt_{max} is the duration of maximum resistance factor in minute; t_v is the LF vibrating time.

In the foam drive process, as the foam liquid is consumed, foaming speed would gradually decrease. When the foaming speed is higher than the defoaming speed, the bubble number will instantly increase and so will the resistance factor. When the foaming speed is lower than the defoaming speed, the bubble number and the resistance factor will obviously decline. Hence the disturbance added by vibration is the reason causing the enhancement in foam plugging effect. Furthermore, the bubble size is decreased and even more distributed [18], leading to stronger foam strength and extended defoaming process, although the maximum amount of foam is reckoned to be constant as shown in Figure 3. Another key factor promoting the foam flooding stability is probably the increased refoaming ability of in situ foam liquid. After some bubble break, new bubbles are soon generated under vibration. In addition, the decreased surfactant consumption for absorption or retention due to LF vibrating might also play a role in extending the duration [19]. Therefore, vibrating time should be prolonged as much as possible when the foam drive is applied in combination with LF vibration technology in field tests.

Vibrating Frequency

It could be noticed in Figure 5 that the resistance factor has shown different tendency for various vibration frequencies. With the increase of vibrating frequency, the MRF becomes larger firstly and then decreases' an optimum value is observed nearby 10 Hz, which indicates a relatively better foam behavior. For a while after foam injection, increased foaming

speed because of a higher frequency shock has improved the foam strength and the plugging efficiency, resulting in a larger value in MRF. However, the faster the oscillation is, the quicker the bubble quantity is decomposed and displaced by subsequent water per unit time. A rapid reduction of foam liquid amount in situ and a smaller resistance factor at the third stage of foam behavior appear under faster oscillation. Nevertheless, an opposite tendency is observed with the DMRF (Figure 6).
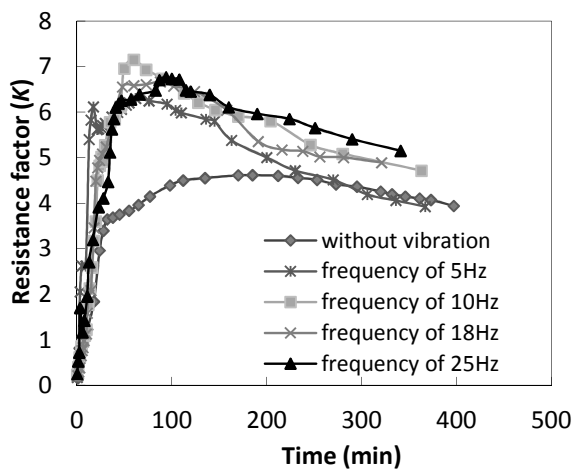

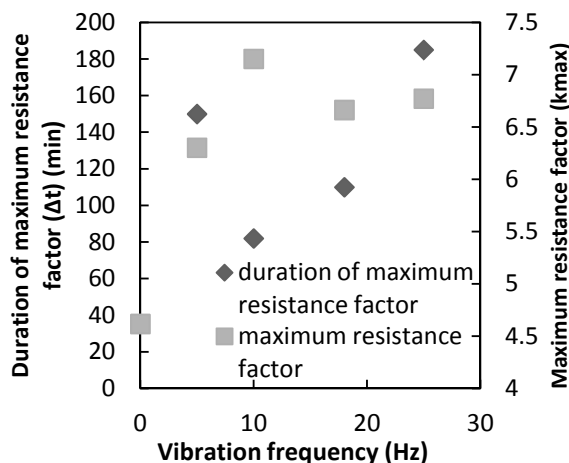**Figure 5: Influence of vibration frequency on foam flooding resistance factor**

Figure 6: Influence of vibration frequency on the maximum resistance factor and its duration

A larger foaming speed is obtained at a higher vibrating frequency. Correspondingly, the foam is not only of a poor foaming capacity but it also has a low breaking rate under LF vibration.

Therefore, a larger value of DMRF is achieved in relatively higher or lower vibrating frequency ranges. In a comprehensive view of MRF and DMRF versus vibrating frequency, an optimal vibrating frequency (10 Hz in the current work) should be considered to improve the comprehensive foam flooding effect in oil field tests.

Vibrating Acceleration

The alterations of resistance factor over time at different vibrating accelerations are not identical (Figure 7); the MRF and its duration also follow similar trends. As shown in Figure 8, MRF increases at first and then decreases as vibrating acceleration increased in the range of 0 to 1.0 m/s^2, with a peak achieved at 0.4 m/s^2. It indicates that at the above optimal vibration the largest foaming speed is obtained and the critical amplitude leads to the largest apparent relative velocity of solid-foam phase and solid-water phase. Following above, a rapid decline in resistance factor, as well as relatively reduced foam stability, appears due to the increase of foam liquid consumption.
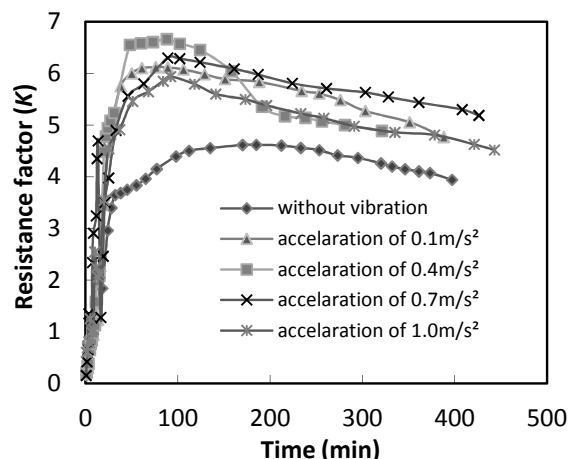

Figure 7: Influence of vibration acceleration on foam flooding resistance factor

Considering the overall performance in foaming and stability, the optimal water plugging effect is observed at acceleration of 0.7 m/s^2. The MRF at acceleration of 0.7 m/s^2 is slightly smaller

than the one at acceleration of 0.4 m/s^2, but the DMRF of the former acceleration is far more than that of the latter. The experiments have shown that proper vibrating acceleration should be seriously selected in oilfield tests for vibration coupling foam injection in order to further enhance the foam displacement efficiency and oil recovery.
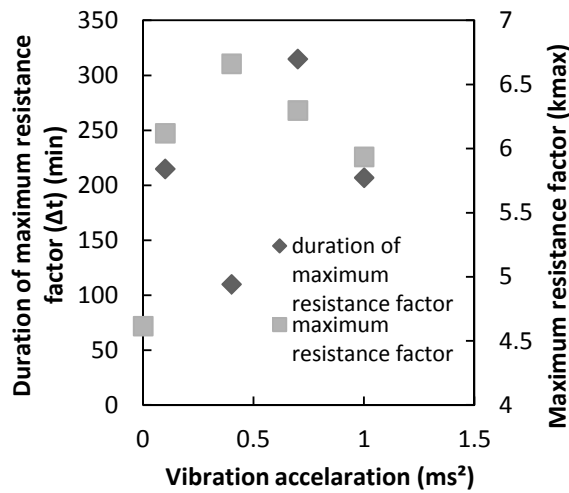

Figure 8: Influence of vibration acceleration on the maximum resistance factor and its duration

FOAM FLOODING MODELING

Foam Flooding Model under LF Vibration

Different from the usual model of foam flooding, the motion equation of foam flooding model under LF vibration needs to take the influence of FSI and the mass conservation equation into consideration.

In the foam flooding model under LF vibration, the following assumptions are made:

1. multiphase and multiple components are included;

2. the gas dissolved in water is not taken into account;

3. only the water phase contains the surfactant, and the influence of surfactant on the density and viscosity of each phase is omitted;

4. the injected fluid percolating in porous media obeys the generalized Darcy's law;

5. the wave attenuation is negligible;

6. the heat transfer and change in the foam flooding process are not considered.

Based on the theory of elastic wave propagation in elastic porous media containing multiphase fluid, the motion equation under the LF vibration of phases as matrix, foam liquid without bubbles (water phase), oil, free gas, and the foam (gas+liquid) is defined by Equation 2 [20-21]:

$$\begin{cases} \nabla \tau_{ij,i} = \rho \ddot{\mathbf{u}}_i + \sum \rho_m \ddot{\mathbf{v}}_{m,i} \\ P_{m,i} = \rho_m \left(\ddot{\mathbf{u}}_i + \ddot{\mathbf{v}}_{m,i} / \phi S_m \right) + \eta_m \ddot{\mathbf{v}}_{m,i} / \kappa_m \end{cases} \tag{2}$$

where τ_{ij} is the total stress and expressed as $\tau_{ij} = \lambda e \delta_{ij} + 2\mu\varepsilon_{ij} - \alpha\delta_{ij}P$ in unsaturated porous media; $P_{m,i}$ is the fluid pressure of component i in phase m; $\mathbf{u}_i$, $\overline{\mathbf{v}}_{w,i}, \overline{\mathbf{v}}_{o,i}, \overline{\mathbf{v}}_{g,i}, \overline{\mathbf{v}}_{f,i}$ is the displacement of the matrix phase, water phase, oil phase, free gas phase, and foam phase respectively; the relative displacement of mobile phase is;

$$\frac{\partial \mathbf{v}_{m,i}}{\partial t} = \phi S_m \left(\frac{\partial \overline{\mathbf{v}}_{m,i}}{\partial t} - \frac{\partial \mathbf{u}_i}{\partial t} \right) \tag{3}$$

S_m represents the saturation of the mobile phase; ρ, ρ_m, and ρ_s are the densities of porous media, fluid, and skeleton respectively. η_m stands for the viscosity of fluid and ϕ is the porosity;

$$\rho = \phi \sum S_m \rho_m + (1-\phi)\rho_s \tag{4}$$

Based on the relationship of the strain, porosity and pore pressure in Biot theory, the constitutive equation is defined as follows:

$$d\phi = \alpha de + \frac{dP}{Q} \tag{5}$$

where e is the volume strain of the rock; P is the confining pressure on solid particles, and is expressed as $P = \sum S_m P_m$ with the average

volume method; $\dfrac{1}{Q}$ is the positive coefficient representing the fluid compressibility under fluid-solid interaction; α is an equivalent representing the action of shear stress on porous media.

The mass conservation equation of component i in phase m is given by Equation 6 [16, 22-24]:

$$\sum_{m=1}^{Np} \nabla \left[\rho_m x_{I,m} \mathbf{v}_m \right] + \phi \sum_{m=1}^{Np} \nabla \left(D_{I,m} \rho_m \nabla x_{I,m} \right) +$$

$$\sum_{m=1}^{Np} q_m x_{I,m} + \phi \sum_{K=1}^{Nr} \left(r_{g,K} - r_{c,K} \right) =$$

$$\frac{\partial}{\partial t} \left(\phi \sum_{m=1}^{Np} \rho_m S_m x_{I,m} \right) + \tag{6}$$

$$\frac{\partial}{\partial t} \left[(1-\phi) \rho_r C_{I,r} \right], I = 1, 2, \cdots, N$$

where $\mathbf{v}_m$ stands for the velocity of mobile phase and expressed in Darcy motion equation as;

$$\mathbf{v}_m = \frac{k k_{rm}}{\mu_m} \left(\nabla P_m - \nabla P_{cm} - \gamma_m Z \right) \tag{7}$$

k is the absolute permeability of reservoir and k_{rm} represents the relative permeability; $x_{I,m}$ means the mole fraction of component I in phase m; μ_m, P_m, P_{cm}, γ_m, q_m, and Z represent the viscosity, reservoir pressure, capillary pressure, specific gravity of overlying rock, source term, and reservoir vertical depth respectively. $r_{g,K}$ and $r_{c,K}$ mean the generation rate and dissipation rate of component I in the physical or chemical reaction K respectively, which is mainly used for the foam phase and could be expressed by the semi-quantitative formula or experimental model formula; Np is the number of phases.

The parameters like viscosity or relative permeability in the foam phase could be expressed as a function of the ones in the gas phase as given below, which is a common approach in foam injection modeling:

$$\mu_f = \mu_g + \frac{\alpha \rho_{ff}}{v_f^{1/3}} \tag{8}$$

$$k_{rf} = k_{rg} \left(S_w \right) \cdot F_M \tag{9}$$

where ρ_{ff} is the density or bubble number per unit volume of gas in flowing foam, not including the foam captured; F_M stands for a dimensionless factor which is related to the maximum foam resistance factor K_{max}, concentration of foaming agent, oil saturation, saturation and velocity of flowing foam, and so on.

The state equation of foam flooding model under LF vibration is identical to the one obtained without LF vibration as given in Equations 10-12, including capillary force formula, saturation normalization, and component normalization.

$$P_{cwo} = P_o - P_w, \ P_{cwg} = P_g - P_w \tag{10}$$

$$S_w + S_o + S_g + S_f = 1 \tag{11}$$

$$\sum_{I=1}^{Nc} x_{I,m} = 1, m = 1, 2, \cdots, N_p \tag{12}$$

Firstly, one may substitute the physical equation, state equation, and the fluid relative displacement of the momentum conservation equation into the continuity equation; then, by removing the item of $d\phi$ from the continuity equation and differentiating with respect to time, the seepage continuity equation of pore fluid is obtained. Based on the solution of simultaneous equations containing the seepage continuity equation, momentum conservation equation, and stress-strain equation in unsaturated porous media, the displacement and seepage rate of multicomponent systems would be obtained.

Bubble Creation and Destruction under LF Vibration

To demonstrate the influence of LF vibration,

the change of bubble generation rate and bubble break rate is analyzed. According to the experimental static performance of foam under LF vibration [12] and expressions about bubble generation [25-26], the foaming speed r_g increases with higher relative velocities of solid-foam phase and solid-water phase v_w and v_f under LF vibration.

$$r_g = k_1^0 v_w v_f^{1/3} \left[1 - \left(\frac{n_f}{n^*} \right)^w \right]$$ (13)

where r_g is the bubble generation rate; k_1^0 is a constant for bubble generation; v_w, v_f, n^*, and w, are water phase velocity, velocity of flowing foam, an upper limit value of foam density, and a constant determined by experiment respectively. Vibration is known to increase fluid seepage velocity; therefore v_w and v_f will increase under vibration and so will the bubble generation rate.

The reasons causing bubble break include gas expansion and gas diffusion, etc. With the analysis of experimental foam performance and expression about bubble break rate (Equation 14) [27-28], the break rate decreases and the foam half-life decomposition extends under LF vibration.

With the impact of shock, the foam size is smaller and evenly distributed; therefore, the sum of liquid membrane surface area and boundary surface area has decreased; the bubble internal break rate (left side of the formula below) also drops, which is related to bubble break due to gas expansion.

$$\left(\frac{d\varepsilon_F}{d\tau} \right) = \frac{1}{V_F} \frac{dA}{d\tau} = \frac{1}{V_F} \left(\frac{dA_f}{d\tau} + \frac{dA_b}{d\tau} \right)$$ (14)

where ε_F is the specific area of the bubble; τ and V_F represent time and foam volume respectively; A is the sum of liquid membrane

surface area (A_f) and boundary surface area (A_b), i.e. $A = A_f + A_b$.
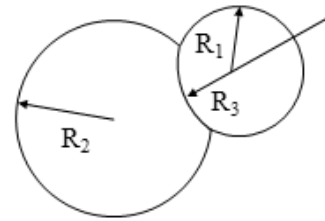

Figure 9: Membrane schematic diagram between two contacted polyhedral bubbles of different radius

The more evenly distributed bubbles (a smaller difference between diameters $|R_2 - R_1|$ of the adjacent bubbles shown in Figure 9) and a decreased contact angle on surfactant solution membrane will cause the curvature radius R_3 of sharing parts between adjacent membranes to increase under LF vibration. Expression about the radius of the sharing membrane between two bubbles of different diameters is detailed as given below. An increased membrane radius R_3 and a decreased specific area ε_F of polyhedral bubble will result in a decrease in the differential pressure P_G' between adjacent bubbles. Gas diffusion, transfer between bubbles, and the value of gas diffusion coefficient (D) all decline. We assume that the parameters (such as degree of bubble number decline due to gas transfer, ambient temperature, the solubility of gas in foam liquid, interfacial tension, and external pressure) remain constant under vibration or without vibration. According to model of De Vrise [27], the bubble break rate caused by gas diffusion and transfer will decrease and the time for generating a certain number of new bubbles will extend as gas diffusion coefficient decreases under LF vibration.

$$R_3 = \frac{2R_1 R_2}{R_2 - R_1} \cos\theta$$ (15)

$$P_G' = P_G - P_o = \frac{2}{3} \sigma \varepsilon_F \frac{n}{n-1} + \frac{\rho g z}{n}$$ (16)

$$\frac{N_t}{N_0} = 1 + K_D' t = 1 + \frac{4RTD\beta\sigma}{P_0 h} t \qquad (17)$$

where R_1 and R_2 are the radius of two adjacent bubbles; θ, R_3, P_G', σ, and n are contact angel on surfactant solution membrane, the curvature radius of sharing parts between adjacent bubbles, the differential pressure between adjacent bubbles, the interfacial tension of solution, and the dimensions of polyhedron respectively; D, R, $\frac{N_t}{N_0}$, P_0, T, and β represent gas diffusion coefficient, the universal gas constant, the degree of bubble number decline due to gas transfer, the external pressure, the ambient temperature, and the solubility of gas in foam liquid respectively.

In summary, the foaming speed increases, but the bubble break rate caused by internal expansion and gas diffusion decreases under LF vibration.

Potential for Application in Low Permeability Reservoirs

Through the research on air foam performance in dynamic displacement under LF vibration, the potential for the application of LF vibration coupling foam drive in low permeability reservoirs is embodied in the following aspects:

(1) Increasing the plugging efficiency of air foam flooding: air foam performance for water plugging under the conditions of vibration has been obviously enhanced. The MRF is increased by about 1.5 times in this paper. The MRF is influenced by the vibrating frequency and acceleration instead of the vibrating time.

(2) Extending the valid time of air foam flooding: the entire process for bubble break and foam liquid consumption, as well as the valid time of air foam flooding, is expanded under vibration; this has already been proved by the experimental results for static foam half-life change under a

resonance wave. Because the actual formation is far greater than indoor experimental model, the property for the extended valid time of foam flooding will be more obvious.

(3) To a certain extent, improving the safety in air injection. With the extended valid time, more gas retention and consumption will be achieved, when the foam is displaced in the underground reservoir. Particularly, when air is injected as a source of foam generation in low-temperature shallow reservoirs, low-temperature oxidation between crude oil and O_2 will be improved; this is indeed good news for providing a way to increase the safety and adaptability of air injection techniques [29-31]. It is a new, albeit important, research direction for improving the development efficiency in air foam flooding and controlling the oxygen concentration from the production well lower than the explosion limit through optimization with the injection parameters or changing the injection technology.

It should be noted that, although the test is carried out with air as a gas source, it does not mean that a specific effect barely exists in air foam flooding under LF vibration and it is the potential for foam flooding with other kinds of gases as the gas source.

CONCLUSIONS

Under LF vibration, air foam performance in dynamic displacement experiments was studied and it was found out that resistance factor under vibration increased by 1.5 times and the valid time was obviously extended. Optimal vibrating frequency and acceleration, resulting in the best foam plugging efficiency, were obtained.

With the analysis of bubble generation and burst rate, foaming speed increased, but foam break rate caused by internal expansion or by gas diffusion and transfer decreased under LF vibration. Dimensionless maximum resistance

factor and dimensionless duration of maximum resistance factor revealed a stronger influence of maximum foaming speed than in situ foam stability.

LF vibration oil extraction technology could enhance the plugging efficiency, extend the valid time, and improve the safety and adaptability of air foam flooding to a certain extent.

ACKNOWLEDGEMENTS

REFERENCES

[1] Zhu Y. Y., Hou Q. F., and Weng R., "Recent Progress and Effect Analysis of Foam Flooding Field Tests in China," *SPE 165211-MS*, **2013**.

[2] Farajzadeh R., Andrianov A., and Krastev R., "Foam-oil Interaction in Porous Media: Implications for Foam Assisted Enhanced Oil Recovery," *Advances in Colloid and Interface Science*, **2012**, *183-184*, 1-13.

[3] Liao J. H., Sun L., and Jiang S. X., "Research and Application of Seismic Shooting Oil Recovery," *Drilling & Production Technology*, **2003**, *5*, 56-58.

[4] Miao X. M., Zheng L. G., and Chen G., "Discussion of Feasibility of Vibration Stimulation Technology by Low-frequency Wave in the Low Permeability Oilfield," *SINO-GLOBAL ENERGY*, **2010**, *12*, 57-59.

[5] Kurawle I., Kaul M., and Mahalle N., "Seismic EOR- The Optimization of Aging Water Flood Reservoirs," *SPE 123304*, **2009**.

[6] Ariadji T., "Effect of Vibration on Rock and Fluid Properties: on Seeking the Vibroseismic Technology Mechanisms," *SPE 93112*, **2005**.

[7] Sun R. Y. and Cheng G. X., "Effect of Artificial Vibration on Liquids Flow through Porous Media," *Journal of Hydrodynamics*, **2004**, *19*(4), 552-557.

[8] Ma J. G., Jin Y. H., and Zhou S. P., "Experiments on the Effects of Mechanical Vibration on Core Permeability," *Journal of Xi'an Shiyou University (Natural Science Edition)*, **1996**, *11*(5), 8-15.

[9] Teng L., Zhaoming Li., and Jing Li., "A Mathematical Model of Foam Flooding Based on Foam Microscopic Seepage Characteristics," *Chinese Journal of Computational Physics*, **2012**, *29*(4), 519-524.

[10] Solbakken J. S., Skauge A., and Aarra M. G., "Supercritical CO_2 Foam - The Importance of CO_2 Density on Foams Performance," *SPE 165296-MS*, **2013**.

[11] Sheng Q., Guo P., and Chen J., "Research on Visual Characteristics of Foam in Porous Media," *Special Oil and Gas Reservoirs*, **2012**, *19*(4), 122-125.

[12] Zhang Lei., "Low-frequency Resonant Wave N_2 Foam Flooding Effect of the Influence of Experimental Study," Xi'an: Xi'an Shi You University, **2012**.

[13] Ashoori E., Marchesin D., and Rossen W. R., "Roles of Transient and Local Equilibrium Foam Behavior in Porous Media: Traveling Wave Original Research Article," *Colloids and Surfaces A: Physicochemical and Engineering Aspects*, **2011**, *377*(1–3), 228-242.

[14] Gong L., Kyriakides S., and Triantafyllidis N., "On the Stability of Kelvin Cell Foams under Compressive Loads Original Research Article," *Journal of the Mechanics and Physics of Solids*, **2005**, *53*(4), 771-794.

[15] Petel O. E., Ouellet S., and Higgins A. J., "The Elastic–plastic Behavior of Foam under Shock Loading," *Shock Waves*, **2013**, *23*(1), 55-67.

[16] Yu H. M., Ren S. R., and Zuo J. L., "Experiment of Improved Oil Recovery by Air Foam Injection Low Temperature

Oxidation Process," *Journal of China University of Petroleum (Edition of Natural Science)*, **2009**, *33*(4), 94-98.

[17] Zhao J. S., Zhang M., and Li T. T., "Study on the Influential Factor of Foam Filtrational Resistance Factor Based on Uniform Design Method," *DRILLING & Production Technology*, **2009**, *32*(4), 74-76.

[18] Bouix R., Viot P., and Lataillade J. L., "Polypropylene Foam Behavior under Dynamic loadings: Strain Rate, Density and Microstructure Effects," *International Journal of Impact Engineering*, **2009**, *36,* 329–342.

[19] Liu J., Pu C. S., and Zheng L. M., "Research on Oil Recovery Technology of Surfactant Flooding Assisted by Low Frequency Resonance Wave," *Oil Drilling & Production Technology*, **2012**, *34*(5), 87-94.

[20] Berryman J. G., Thigpen L., and Chin R., "Bulk Elastic Wave Propagation in Partially Saturated Porous Solids," *Acoust. Soc. Amer*, **1988**, *84*, 360-373.

[21] Cai Y. Q., Li B. Z., and Xu C. J., "Analysis of Elastic Wave Propagation in Sandstone Saturated by Two Immiscible Fluids," *Chinese Journal of Rock Mechanics and Engineering*, **2006**, *25*(10), 2009-2016.

[22] Kam S. I., Nguyen Q. P., and Rossen W. R., "Dynamic Simulations with an Improved Model for Foam Generation," *SPE Journal*, **2007**, *3*, 35-48.

[23] Li S. Y., Li Z. M., and Li B. F., "Experimental Study and Application on Profile Control Using High Temperature Foam," *Journal of Petroleum Science and Engineering*, **2011**, *78*(3-4), 567-574.

[24] Li S. Y., Li Z. M., and Li B. F., "Experimental Study of Effect of Permeability on Foam Diversion," *Petroleum Sci. and Tech.*, **2012**, *30*(18), 1907-1919.

[25] Falls A. H., Gauglitz P. A., and Hirasaki G. J., "Development of a Mechanistic Foam Simulator: The Population Balance and Generation by Snap-off," *SPE 14961*, **1986**.

[26] Yu H. M., Ren S. R., and Zuo J. L., "A Mathematical Model and Numerical Simulation Method for Air-foam Flooding," *Acta Petrolei Sinica*, **2012**, *4*, 653-657.

[27] Exerowa D. and Kruglyakov P. M., "Foam and Foam Films: Theory, Experiment, Application," Elsevier, **1998**.

[28] Pinazo A. P., Infante M. R., and Frances E.I., "Relation of Foam Stability to Solution and Surface Properties of Gemini Cationic Surfactants Derived from Arginine," *Colloids and Surfaces A*, **2001**, *189*, 225-235.

[29] Alvarez J. M., Rivas H. J., and Rossen M. R., "Unified Model for Steady Sate Foam Behavior at High and Low Foam Qualities," *SPE 56825*, **1999**.

[30] Dong X., Liu H., and Sun P., "Air-foam-injection Process: An Improved-oil-recovery Technique for Waterflooded Light-oil Reservoirs," *SPE Reservoir Evaluation & Engineering*, **2012**, *15*(4): 436-444.

[31] Dong X. H., Liu H. Q., and Pang Z. X., "Study on Reaction Kinetics of Low Temperature Oxidation of Air Injection in Light Crude Oil," *Applied Chemical Industry*, **2012**, *41*, 1135-1139.